

ON THE FREQUENCY-PERIOD DISTRIBUTION OF GALACTIC CEPHEIDS

A. Serrano

Instituto de Astronomía
Universidad Nacional Autónoma de México

Received 1983 March 9

RESUMEN

Se analiza la distribución del número de cefeidas galácticas como función del período. La distribución observada muestra que tanto la densidad de cefeidas como el período, P_1 , del máximo de la distribución, y la anchura de ésta varían con la distancia galactocéntrica. De una comparación entre las distribuciones teóricas y observacionales, se han derivado restricciones a los modelos de evolución estelar y al ancho de la banda de inestabilidad. Suponiendo la función inicial de masa de Serrano (1978), se encuentra que: a) las cefeidas galácticas no muestran evidencia de que exista una tasa bimodal de formación estelar, con una mayor amplitud para masas grandes, b) las cefeidas con períodos mayores que P_1 , permanecen como cefeidas por un tiempo que varía como $P^{-0.65}$, c) la tasa de formación estelar (TFE) en la vecindad solar es de 1.2 estrellas $\text{pc}^{-2} \text{G año}^{-1}$, d) el gradiente local de la abundancia de elementos pesados, Z , es de $\nabla \log Z = -0.12 \text{ kpc}^{-1}$, e) el gradiente local de la TFE es $\nabla \log \text{TFE} = -0.16 \text{ kpc}^{-1}$.

ABSTRACT

An analysis is made of the frequency-period distribution of galactic Cepheids. The observed distribution shows that the density of Cepheids, the period, P_1 , of the maximum and the width of the distribution vary with galactocentric distance. From a comparison with the theoretical distribution constraints on the stellar evolutionary models and on the width of the instability strip are derived. Assuming Serrano's (1978) IMF it is shown that: a) in the case of the Galaxy, Cepheids show no evidence for a two component birthrate with higher amplitudes for large masses, b) for Cepheids with period longer than P_1 , the lifetime as a Cepheid varies as $P^{-0.65}$, c) the star formation rate, SFR, in the solar neighborhood is 1.2 stars $\text{pc}^{-2} \text{Gyr}^{-1}$, d) the local gradient of heavy elements abundance, Z , is $\nabla \log Z = -0.12 \text{ kpc}^{-1}$, e) the local gradient of SFR is $\nabla \log \text{SFR} = -0.16 \text{ kpc}^{-1}$.

Key words: STARS-CEPHEIDS

I. INTRODUCTION

The frequency-period distribution for classical Cepheids has been studied by Hofmeister (1967) and by Becker, Iben, and Tuggle (1977). Assuming that Cepheids are in the phase of core helium burning these authors have produced theoretical distributions with a short-period cutoff and a maximum. Furthermore, Hofmeister pointed out, and Becker *et al.* proved quantitatively, that the position of the maximum is a function of chemical composition.

Becker *et al.* (1977) have compared the theoretical distributions with the observed ones in seven galaxies of the Local Group. They find that the short-period cutoff and the maximum peak in the distributions occur at successively larger values of $\log P$ when galaxies are ordered according to their heavy-element abundance, Z . The theoretical distributions obtained by Becker *et al.* also show the cutoff and the maximum increasing with Z .

However, when comparing in detail the distributions, Becker *et al.* (1977) concluded that in the observed frequency-period distribution there is an excess of longer period Cepheids which could only be explained by

adopting a two component birthrate function. The secondary component, that of the massive stars, would have an amplitude 5 to 50 times greater than the primary background.

It has long been known (Shapley and McKibben 1940; van den Bergh 1958; Baade and Swope 1965; Fernie 1968) that in galaxies of the Local Group, short period Cepheids are concentrated towards the outer regions of the galaxy and long-period Cepheids towards the inner regions. In the case of the Galaxy, Fernie (1968) finds that the average period decreases with galactocentric distance at the rate of about 1 day kpc^{-1} .

It is the purpose of this paper to show that the excess of long period Cepheids in the galactic frequency-period distribution may be explained by a gradient of the star formation rate (SFR) combined with a gradient in metal abundance.

In order to do this, the observed and theoretical frequency-period distributions are re-examined in §II and §III, respectively. Moreover, in §III it is shown that the distribution is specified by three parameters: the period, P_1 , of the maximum of the distribution; the short-period

cutoff, P_0 , and the rate at which Cepheids with periods longer than P_1 decay in number with respect to the period.

A comparison between observation and theory is presented in §IV. It is discussed how P_1 depends mainly on Z . This allows an estimation of the local gradient of Z to be made; the relation between the long period tail of the distribution and the lifetime of a Cepheid as a function of period is discussed; the relation between the width of the instability strip and the loci of the bluest points during core helium burning is examined and the local values of the SFR and of its radial gradient are obtained.

II. THE OBSERVED FREQUENCY-PERIOD DISTRIBUTION

The first problem one encounters when trying to construct a frequency-period distribution for galactic classical Cepheids is that catalogues of these variables are highly incomplete. Fernie (1968), for example, analyzed the catalogue by Fernie and Hube (1968) and concluded that at 4 kpc the surveys were more than 80% incomplete.

In order to take into account this incompleteness, I selected only Cepheids from the General Catalogue of Variable Stars (Kukarkin *et al.* 1958) with distances less than 5 kpc from the sun (285 stars) as given by Fernie and Hube (1968). As these authors argue, stars with distances greater than 400 pc from the galactic plane are probably not classical Cepheids. So, I have further restricted the sample to those stars with $|z| < 400$ pc (275 stars). If these 275 stars are divided into four quadrants centered at galactic longitudes 0° , 90° , 180° , and 270° , respectively, then it is possible to derive the surface density of Cepheids as a function of distance from the sun, for each of the four quadrants.

The resulting density profiles, normalized in each case to the density within 1 kpc, have some conspicuous characteristics. Firstly, the density of Cepheids decreases, in all directions, as the distance from the sun increases. This effect, for the whole sample has been pointed out by Fernie (1968), and is undoubtedly due to incompleteness. Secondly, the density profile towards the galactic center diminishes much more rapidly than in any other direction. Thirdly, the Cepheids with periods between 4 and 10 days have the same density profile (within 20%) in each of the quadrants outside the direction of the galactic center. On the contrary, Cepheids with $P < 4$ days or $P > 10$ days show very different density profiles in each quadrant. Fourthly, when the distance from the sun is greater than 4 kpc the density has diminished, in the best of cases, by more than a factor of three.

Figure 1 shows the density profile of Cepheids with periods between 4 and 10 days as a function of distance from the sun, for two cases: in the direction of the galactic center, and for an average of the other 3 quadrants. As discussed later, some true decrease in the density of Cepheids is expected in the direction of the galactic center, thus, I have adopted the average density profile of the three quadrants outside the direction of the center as

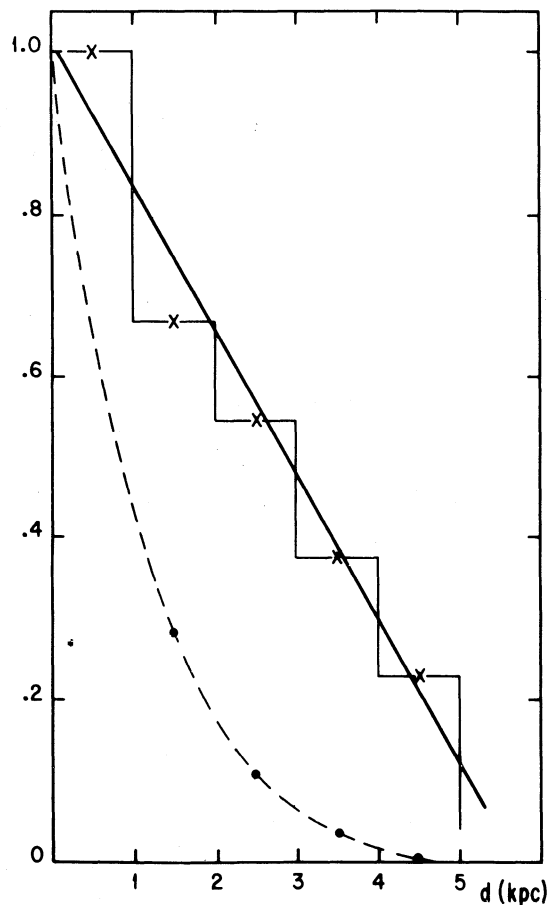


Fig. 1. Density profile of Cepheids with periods between 4 and 10 days, as a function of the distance from the sun normalized to the density within the first kpc. Broken line corresponds to quadrant in the direction of the center; histogram and continuous line correspond to an average of 3 quadrants outside the center.

representative of the whole sample. This average density profile is represented by the solid line in Figure 1.

A corrected space distribution of Cepheids is constructed by weighting each Cepheid at a distance d from the sun by the inverse of the density profile at d . In this way, the density of intermediate period Cepheids outside the galactic center, is forced to be approximately constant with d . Using this correction scheme each Cepheid at a distance between 4 and 5 kpc would have a weight between 3 and 10; to maintain the correction factors as small as possible, we have arbitrarily excluded these stars, and we considered only those variables at a distance less than 4 kpc from the sun, 232 stars, which have density corrections less than a factor of three.

In order to study radial variations across the galaxy, the whole sample has been divided into three subsamples having galactocentric distances, R , in the range 7-9 kpc, 9-11 kpc and 11-13, respectively. By this procedure the number of stars comes down to 222.

For each of the radial subgroups a frequency-period distribution has been constructed by dividing the log P axis between 0 and 1.5 (1 day to 30 days) in intervals of width 0.1 in log P and by calculating the surface density of Cepheids in each period interval.

Since different areas are sampled in each case, the surface density of Cepheids in the i -th period interval, σ_i' , has been calculated in two ways. Firstly, by dividing the total number of Cepheids in that interval by the total area in question; and secondly by subdividing the area into regions bounded by circles around the sun and around the galactic center separated by 1 kpc each, calculating the surface density of Cepheids in each region, and taking the average over the different subareas. The two methods of calculation yield distributions that differ by less than 10%. Consequently, the average of the two methods has been taken as the true distribution.

Finally to attenuate the effects of binning, the frequency-period distribution σ_i' has been smoothed by taking

$$\sigma_i = (\sigma_{i-1}' + 2\sigma_i' + \sigma_{i+1}')/4$$

as the density of Cepheids in the i -th interval.

The resulting distributions, for each R interval, are

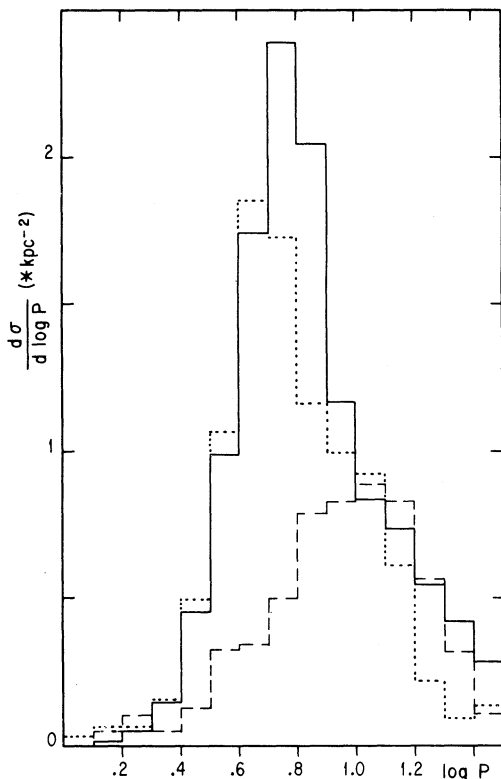


Fig. 2. Frequency-period distribution of galactic Cepheids. Dashed, continuous and dotted line histograms correspond to Cepheids with galactocentric distances between 7-9, 9-11 and 11-13 kpc, respectively.

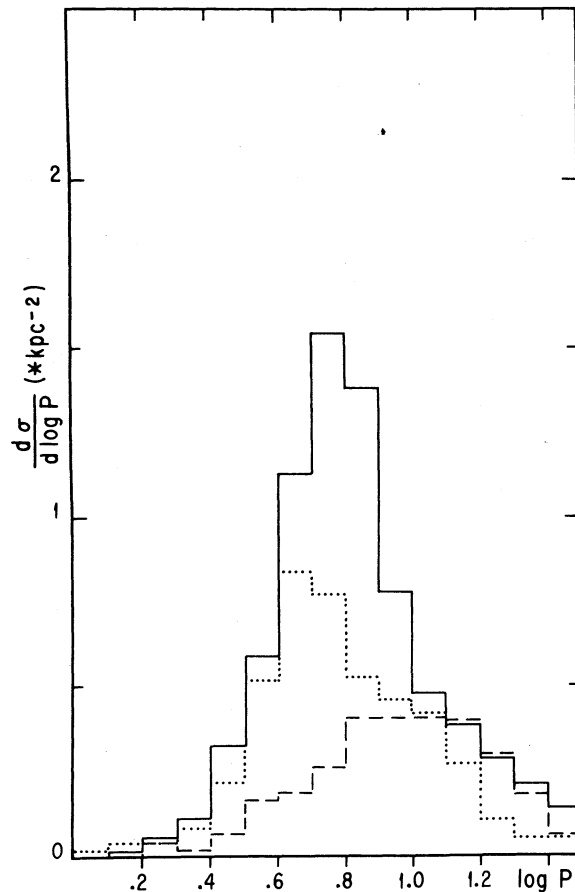


Fig. 3. As in Figure 2, but with no correction for incompleteness.

shown in Figure 2. For a comparison, the distributions with no correction for incompleteness are shown in Figure 3.

To my knowledge it is the first time that the frequency-period distributions have been calculated in a correct form because effects of incompleteness are taken into account in a distance limited sample, and because the surface density of Cepheids and not the total number is calculated for each period interval.

III. THE THEORETICAL FREQUENCY-PERIOD DISTRIBUTION

It is a well established fact that among stars of intermediate mass there are two sequences in the H-R diagram where stars burn helium in the core (see e.g., review by Iben 1974; Becker *et al.* 1977 and references therein). One sequence roughly coincides with the locus of the red giant branch and the other one intersects the red giant branch at low luminosity and is bluer at higher luminosities. For any given stellar mass core helium burning in the blue takes place at roughly the same luminosity of the red giant tip and corresponds to the bluest point in the evolutionary track. Between these two

stages there is a phase of rapid evolution on a thermal timescale.

The Cepheid instability band crosses, generally speaking, somewhere in the middle of the two core helium burning sequences when the luminosity is high. At lower luminosities the instability strip intersects the sequence of the bluest points at two luminosities: the blue edge at a luminosity L_1 and the red edge at a lower luminosity L_0 (Figure 4). Since Cepheids are believed to be in the phase of core helium burning, they will correspond to the stars, of luminosity greater than L_0 , crossing the instability strip.

The location of the two sequences of core helium burning, the time spent in each region, and the location of the instability strip itself are functions of the chemical composition. To date, the most complete study for different compositions and stellar masses is that by Becker *et al.* (1977). I will try to construct highly simplified theoretical frequency-period distributions based on the models by these authors.

Let $\psi(t)$ be the total stellar birthrate, per unit area and unit time and $\phi(m)$ the initial mass function (IMF),

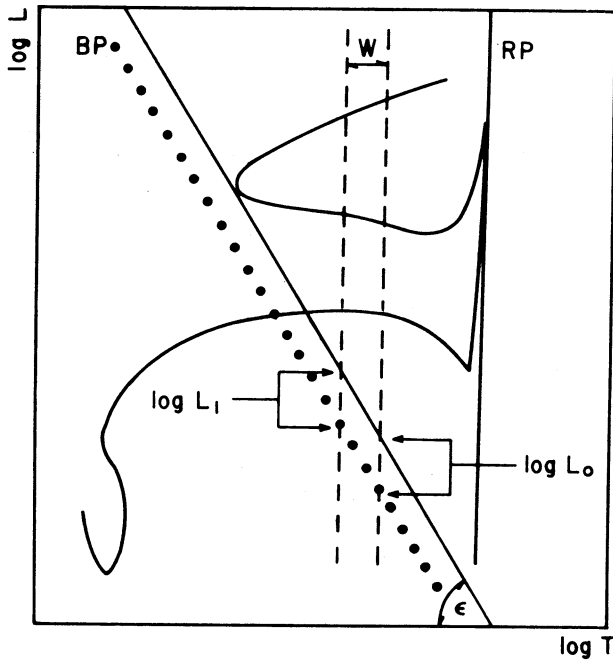


Fig. 4. Schematic representation, in a theoretical H-R diagram, of various aspects discussed in the text. A typical intermediate-mass star evolutionary track is sketched. Helium burning in a nuclear timescale takes place at the tip of the giant branch and at the bluest point in the subsequent evolution. The two sequences of He burning are shown by full lines: the line RP coincident with the tips of the red giant branches and the line BP of the sequence of the bluest points. The instability strip (dashed lines), of width W , intersects the sequence of the bluest points at luminosities L_1 (blue edge), and L_0 (red edge). Also shown the slope ϵ of the BP line, and the bluest-point sequence obtained when the metallicity is decreased (dotted line).

assumed to be independent of time and of chemical composition. Then $\psi(t') \phi(m) dm dt'$ is the number of stars born between t' and $t' + dt'$ and mass between m and $m + dm$. Hence, the number dN of Cepheids with mass between m and $m + dm$ is given by

$$dN = \psi(t - \tau(m)) \phi(m) \Delta t(m) dm ; \quad (1)$$

where $\tau(m)$ is the lifetime of a star from the ZAMS to the edge of the instability strip and Δt is its crossing time of this band.

For all relevant masses $\tau(m) \lesssim 10^8$ y so that we can assume, as Becker *et al.* did, that $\psi[t - \tau(m)] \approx \psi(t)$ and obtain the frequency-period distribution of Cepheids as

$$\frac{dN}{d \log P} = \psi(t) m \phi \Delta t \ln 10 \frac{d \log m}{d \log P} \quad (2)$$

It is clear from equation (2) that to construct a theoretical frequency-period distribution it is necessary to know ψ as a scaling factor, the IMF, and, from stellar evolutionary models, the mass-period relation and Δt the lifetime of a Cepheid as a function of period.

Becker *et al.* (1977) have shown that the first time a star crosses the instability strip from red to blue the theoretical period-luminosity relation is

$$\log L = 2.51 + 1.25 \log P \quad (3)$$

independent of composition. In the case of multiple excursions to the blue, most of the time is spent in this first crossing from red to blue. For simplicity, I shall neglect all other crossing.

For the same stage Becker *et al.* (1977) have obtained a mass-luminosity relation that depends on the helium abundance, Y , and on the heavy element abundance, Z . However, as has been first proposed by Peimbert and Torres-Peimbert (1974) and extensively discussed by Lequeux *et al.* (1979) and by Serrano and Peimbert (1981), Y is related to Z by

$$\Delta Y = Y - Y_p \approx 3 \Delta Z \quad (4)$$

where the pregalactic value of $Y_p \approx 0.228$. Using equations (3) and (4) in the mass-luminosity relation by Becker *et al.* (1977) the composition-dependent mass period relation

$$\log m = \alpha + \beta \log P ; \quad (5)$$

with

$$\alpha = 0.45 + 5.1Z - 10.9 Z^2$$

$$\text{and } \beta = 0.355 - 0.41Z - 8.9 Z^2 \quad (6)$$

Typically, as Z increases, so does the mass corresponding to a given period.

For luminosities larger than L_1 , Δt decreases both because the timescale for core helium burning decreases at higher luminosities and because the region of slow burning goes farther to the blue of the instability strip. Consequently, I shall assume that for $P > P_1$,

$$\Delta t = \Delta t_1 (P/P_1)^{-\gamma} \quad (7)$$

Here subindices 1 refer to the track just touching the blue edge of the instability strip at L_1 (Figure 4).

Cepheids with luminosity less than L_1 have longer core helium burning timescales but also penetrate less into the instability strip as the luminosity decreases; at L_0 they spend no time on it. Let us assume that in this range Δt is proportional to the intrusion into the instability strip. The red edge of the strip is approximately constant in this range and for the bluest points it is obtained from stellar models $\log T \propto \log L$. Thus, I shall take

$$\Delta t = \Delta t_1 \log (P/P_0) / \log (P_1/P_0) \quad (8)$$

for P between P_0 and P_1 . The periods P_0 and P_1 are determined by the intersections of the bluest-point line

$$\log L_{BP} = \delta + \epsilon \log T_{BP} \quad (9)$$

with the blue and red edges of the instability strip.

Inserting equations (3) through (6) into the expression for the blue edge of the instability strip calculated by Iben and Tuggle (1975) we obtain

$$\log T_{BE} = 3.812 + \zeta \Delta \log L + \eta (\Delta \log L)^2 \quad (10)$$

with

$$\begin{aligned} \Delta \log L &= \log L - 3.25 \quad , \\ \zeta &= -0.0466 + 0.3 Z \quad , \\ \eta &= -0.0021 - 0.017 Z \quad . \end{aligned} \quad (11)$$

The strip is assumed to have a constant width W ,

$$W = \log T_{BE} - \log T_{RE} \quad (12)$$

From stellar evolutionary models one can calculate the time $\Delta t^*(L)$ that a star of a given luminosity spends

within an interval W to the red of the bluest point. An estimate of Δt_1 is then $\Delta t_1 = \Delta t^*(L_1)$. From models by Becker *et al.* (1977) and Becker (1981) it is obtained that

$$\Delta t^* = e^{-2.2Z} (L/L^*)^{-0.85} \quad (13)$$

with

$$\log L^* = 4.5 \quad .$$

The IMF by number is given by a power law

$$\phi \propto m^{-1-x} \quad (14)$$

I will use Serrano's (1978) IMF (see e.g., Serrano and Peimbert 1981)

$$m \phi = 0.0714 m^{-2} \quad (15)$$

The theoretical frequency-period distribution is completely determined, up to a scaling factor $\psi(t)$, by δ and γ . Solving first equations (9), (10) and (12), P_0 and P_1 are determined; Δt , then follows from equation (13) and finally the distribution is obtained by inserting equations (5), (15) and (7) or (8) into equation (2). Alternatively, the distribution is completely determined, for a given chemical composition and SFR, if one knows P_0 , P_1 , and γ .

In order to compare theoretical and observed distributions it is necessary to integrate equation (2) over the interval in $\log P$. If the limits of the i -th interval are P_i and P_{i+1} it can easily be shown that

$$\begin{aligned} \Delta N_i &= \int_{\log P_i}^{\log P_{i+1}} dN = \\ &= \{(m \phi \Delta t)_i - (m \phi \Delta t)_{i+1}\} \beta \psi / (\beta x + \gamma) \quad , \end{aligned} \quad (16)$$

for $P_i > P_1$; and

$$\Delta N_i = \{(m \phi \Delta t')_i - (m \phi \Delta t)_{i+1}\} \psi / x \quad , \quad (17)$$

for $P_{i+1} < P_1$, where

$$\Delta t' = \Delta t - \Delta t_1 / \beta x \quad . \quad (18)$$

IV. COMPARISON BETWEEN OBSERVATIONS AND THEORY

a) The Period P_1 of Maximum Frequency

Stellar evolutionary models indicate that if Z is

decreased the bluest-point sequence shifts to the blue (δ decreases in equation 9) and consequently P_1 decreases.

Figure 5 shows the relation between P_1 and Z obtained by Becker *et al.* (1977). The observed points for the Magellanic Clouds and the solar neighborhood are also shown there. P_1 in the Magellanic Clouds has been obtained from data by Payne-Gaposchkin (1970, 1971) and for the solar neighborhood from Figure 1; Z is taken from Lequeux *et al.* (1979).

It is quite evident that at low Z , models predict shorter P_1 than what is actually observed. It must be concluded that low Z stellar models go too far to the blue, especially in the mass range 2 to 4 m_{\odot} . It is well known that the bluest point sequence is a very sensitive function of the hydrogen profile left behind by the receding convective core during the main sequence phase; of the cross section C^{12} (α , γ) O^{16} , of overshoot and semi-convection; of rotation; and of mass loss (see Iben 1974 and references therein). Uncertainties in all these factors make equation (9) the most uncertain result of stellar evolutionary models. Consequently, I shall adopt for the rest of this paper the relation defined by the observed points.

$$\log P_1 = 1.7 + 0.56 \log Z \quad (19)$$

From the observed P_1 values in the galactic distribution presented in Table 1 one can immediately conclude that there is a negative radial gradient of Z in the galaxy:

$$\nabla \log Z = -0.12 \text{ kpc}^{-1} \quad (20)$$

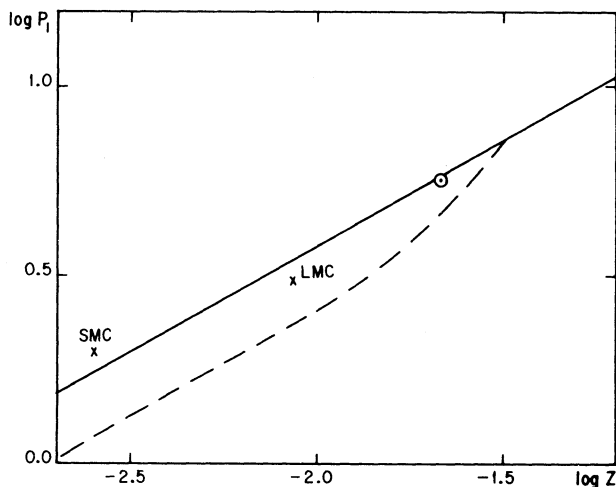


Fig. 5. Period of maximum frequency, P_1 , as a function of heavy elements abundance Z . Continuous line corresponds to equation (19) while dashed line is taken from models by Becker *et al.* (1977). Also shown are the observed values for the Magellanic Clouds and the present solar neighborhood.

This value is to be compared with $\nabla \log Z \approx -0.07 \text{ kpc}^{-1}$ obtained by Harris (1981) from Washington photometry of 102 Cepheids. As this author indicates, if metal-poor stars are bluer at a given period then the derived gradient increases up to $\sim -0.1 \text{ kpc}^{-1}$ which is nearly the same value as we obtain.

A similar value, -0.08 kpc^{-1} , has been obtained by Peimbert (1977) by using the gradient of average period derived by Fernie (1968). The local value of $\nabla \log Z$ derived from H II regions is also -0.08 kpc^{-1} (as in Peimbert 1979, but with $t^2 = 0.02$; see Peimbert and Serrano 1982 for a discussion of this point). This value is also in excellent agreement with the value of $\nabla \log Z$ derived from planetary nebulae (Torres-Peimbert and Peimbert 1977; Peimbert and Serrano 1980). Note also that data suggest that the gradient is steeper in the direction of the galactic center. Carral, Rodríguez, and Chaisson (1981) have obtained, from radio recombination line observations, a similar result.

b) The Short Period Cutoff P_0

From equations (3), (9), and (10) and the definition of P_0 and P_1 a relation can easily be obtained between the slope ϵ , of the bluest point sequence and the width W of the instability strip:

$$\epsilon^{-1} = 0.8 W/D + \zeta + \eta (1.25 \log P_1 P_0 - 1.48) \quad (21)$$

$$\approx 0.8 W/D \quad ,$$

where

$$D = \log P_1 - \log P_0 \quad .$$

Adopting $W = 0.04$ and values of ϵ from Becker *et al.* (1977) one obtains D in the range 0.05 to 0.01. However observed distributions show that, typically, D is in the range 0.3 to 0.6.

The discrepancy can be solved in two ways, either it is assumed that theoretical ϵ , W and D are consistent with equation (21) and the observed D is different because of chemical inhomogeneities, or it is assumed that D is given by the observed value because W and/or ϵ are not well represented by theory.

In the former case, a perfect theory, one obtains from equation (21) that inhomogeneities of Z in star formation typically amount to $\sigma_{\log Z} \approx 0.3$.

In the latter case, when there are no Z inhomogeneities in star formation, one needs to increase the width of the instability strip to $W \sim 0.12$ or to increase the slope, ϵ , of the bluest points sequence to ~ 12 or a combination of both.

It should be noticed that Pel and Lub (1978) and Deupree (1980) have estimated $W \sim 0.15$. For this reason and for the sake of simplicity, I will assume for the rest of the paper that the observed P_0 corresponds to the same chemical composition as the observed P_1 .

c) *The Variation of Lifetime with Period*

From equations (5), (7), and (16) it follows that

$$\Delta N_i \propto P^{-\gamma-\beta x} \quad (23)$$

for Cepheids with $P > P_1$. In this way an observational determination of γ can be made from the slope of the $\log \sigma_i$ versus $\log P$ values. Figure 6 shows a diagram of the observed $\log \sigma_i$ as a function of $\log P$. From this figure it is clear that equation (23) indeed holds, and so that

$$\sigma_i \propto P^\kappa$$

with a slope, κ , in the range -1.10 to -1.50 . Using $\beta = 0.3$ and $x = 2$, these values of κ imply values of γ in the range 0.4 to 0.9 . These values should be compared with values in the range 2 to 5 estimated from models by Becker *et al.* (1977).

The slope γ of the $\log \Delta t$ versus $\log P$ curve is smaller than the theoretical one and is rather similar to the slope of the core helium burning timescale Δt^* given in equation (13). It seems that regions of slow evolution to the blue of the instability strip in the H-R diagram are nearer to this strip than what models predict; this is a further indication that models go too far to the blue. In what follows I have adopted $\gamma = 0.65$, corresponding to the line in Figure 6.

d) *The Star Formation Rate*

In Table 1 a comparison of the basic aspects of observed and theoretical distributions is presented. These include the average and the dispersion of $\log P$ and the density of Cepheids with periods longer than 10 days, relative to the total Cepheid density, σ_T . With the chosen parameters shown in the same table, the agreement between theory and observation for the shape of the distributions is satisfactory.

Notice that there is not a significant excess of long period Cepheids in the observed distributions with respect to the theoretical one. Thus, a two component

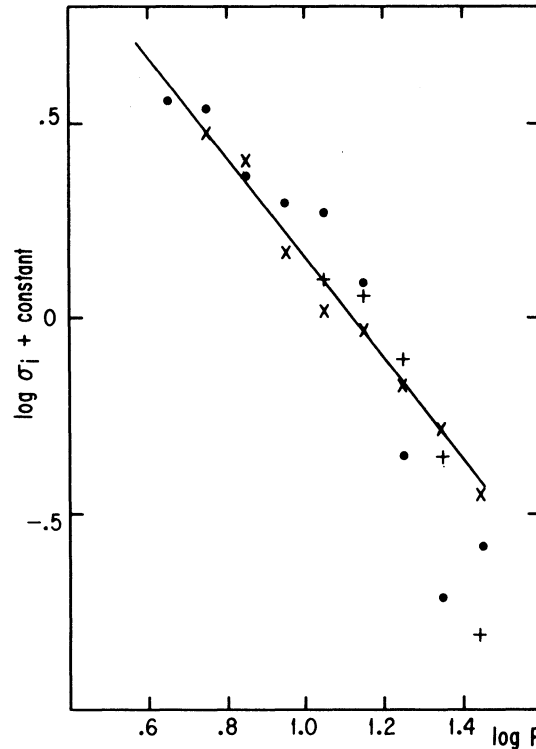


Fig. 6. Logarithm of long period tail of observed distributions, as a function of $\log P$. The line has a slope of -1.25 and corresponds to $\gamma = 0.65$.

birthrate proposed by Becker *et al.* (1977) to explain an overall galactic frequency-period distribution is no longer needed. Further investigation should be made to check this explanation for other galaxies of the local group.

The theoretical distributions give the density per unit SFR, σ_T/ψ . By comparing these values with the total observed densities, values for ψ can be obtained at each galactic radius. A negative gradient of SFR is evident, with a value

$$\nabla \log \text{SFR} = -0.16 \text{ kpc}^{-1} \quad ,$$

TABLE 1

PROPERTIES OF OBSERVED VERSUS THEORETICAL FREQUENCY-PERIOD DISTRIBUTIONS^a

R (kpc)	Observed						Theoretical					
	$\log P_0$	$\log P_1$	$\log P$	disp(log P)	$\frac{\sigma(P > 10 \text{ d})}{\sigma_T}$	σ_T (* kpc ⁻²)	$\log P$	disp(log P)	$\frac{\sigma(P > 10 \text{ d})}{\sigma_T}$	$\frac{\sigma_T}{\psi}$ (10 ³ y)	ψ (* pc ⁻² Gy ⁻¹)	
11-13	0.25	0.65	0.79	0.24	0.21	9.53	0.77	0.34	0.19	18.49	0.52	
9-11	0.30	0.75	0.84	0.25	0.24	11.9	0.84	0.35	0.25	9.85	1.21	
7-9	0.35	0.92	0.95	0.27	0.46	5.84	0.96	0.37	0.37	2.52	2.31	

a. Where P is given in days and σ is the surface density of Cepheids.

i.e., it decreases by a factor of two for each 2 kpc. This value as in agreement with the values obtained from supernovae remnants (Kodaira 1974), pulsars (Taylor and Manchester 1977; Guibert, Lequeux, and Viallefond 1978), and H II regions (Mezger and Smith 1977; Mezger 1978).

Moreover, the local value of the SFR obtained in this way: $1.2 \text{ star pc}^{-2} \text{ Gy}^{-1}$ is in excellent agreement with the values derived by Serrano (1978), Miller and Scalo (1979) and Twarog (1980).

REFERENCES

- Baade, W. and Swope, H. 1965, *A.J.*, 70, 212.
 Becker, S.A. 1981, *Ap. J. Suppl.*, 45, 475.
 Becker, S.A., Iben, I. Jr., and Tuggle, R.S. 1977, *Ap. J.*, 218, 633.
 Carral, P., Rodríguez, L.F., and Chaisson, E.J. 1981, *Astr. and Ap.*, 95, 388.
 Deupree, R.G. 1980, *Ap. J.*, 236, 225.
 Fernie, J.D. 1968, *A.J.*, 73, 995.
 Fernie, J.D. and Hube, J.O. 1968, *Ap. J.*, 73, 492.
 Guibert, J., Lequeux, J., and Viallefond, F. 1978, *Astr. and Ap.*, 68, 1.
 Harris, H.C. 1981, *A.J.*, 86, 707.
 Hofmeister, E. 1967, *Z. Astrophys.*, 65, 194.
 Iben, I., Jr. 1974, *Ann. Rev. Astr. and Ap.*, 12, 215.
 Iben, I., Jr. and Tuggle, R.S. 1975, *Ap. J.*, 197, 39.
 Kodaira, K. 1974, *Pub. Astr. Soc. Japan*, 26, 255.
 Kukarkin, B.W., Parenago, P.P., Efremov, Yu., I., and Krolpov, P.N. 1958, *General Catalogue of Variable Stars*, 2nd. edition (Moscow: Academy of Sciences).
 Lequeux, J., Peimbert, M., Rayo, J.F., Serrano, A., and Torres-Peimbert, S. 1979, *Astr. and Ap.*, 80, 155.
 Mezger, P.G. 1978, *Astr. and Ap.*, 70, 565.
 Mezger, P.G. and Smith, L.F. 1977, in *IAU Symposium No. 75, Star Formation*, eds. T. de Jong and A. Maeder (Dordrecht: D. Reidel), p. 135.
 Miller, G.E. and Scalo, J.M. 1979, *Ap. J. Suppl.*, 41, 513.
 Payne-Gaposchkin, C. 1970, *Galactic Astronomy*, ed. H-Y Chiu and A. Muriel (New York: Gordon & Breach), 2, 245.
 Payne-Gaposchkin, C. 1971, *The Magellanic Clouds*, ed. A.B. Muller (New York: Springer-Verlag), p. 34.
 Peimbert, M. 1977, in *IAU Colloquium No. 45, Chemical and Dynamical Evolution of our Galaxy*, eds. E. Basinska-Grzerik and M. Mayor (Dordrecht: D. Reidel), p. 149.
 Peimbert, M. 1979, in *IAU Symp. No. 84, The Large Scale Characteristics of the Galaxy*, ed. W.B. Burton (Dordrecht: Reidel), p. 37.
 Peimbert, M. and Serrano, A. 1980, *Rev. Mexicana Astron. Astrof.*, 5, 9.
 Peimbert, M. and Serrano, A. 1982, *M.N.R.A.S.*, 198, 563.
 Peimbert, M. and Torres-Peimbert, S. 1974, *Ap. J.*, 193, 327.
 Pel, J.W. and Lub, J. 1978, in *IAU Symposium No. 80, The HR Diagram*, eds. A.G. Davis Philip and D.S. Hayes (Dordrecht: D. Reidel), p. 229.
 Serrano, A. 1978, Ph. D. Thesis, University of Sussex.
 Serrano, A. and Peimbert, M. 1981, *Rev. Mexicana Astron. Astrof.*, 5, 109.
 Shapley, H. and McKibben, V. 1940, *Proc. Natl. Acad. Sci.*, 26, 105.
 Taylor, J.H. and Manchester, R.N. 1977, *Ap. J.*, 215, 885.
 Torres-Peimbert, S. and Peimbert, M. 1977, *Rev. Mexicana Astron. Astrof.* 2, 181.
 Twarog, B.A. 1980, *Ap. J.*, 242, 242.
 Van den Bergh, S. 1958, *Ap. J.*, 63, 492.

Alfonso Serrano: Instituto de Astronomía, UNAM, Apartado Postal 70-264, 04510 México, D.F. México.